

Supplementary Material for

Characteristics, origin, and significance of chessboard subgrain boundaries in the WAIS Divide Ice Core

Joan J. Fitzpatrick¹, Larry A. Wilen², Donald E. Voigt³, R.B. Alley³, J.M Fegyveresi⁴

¹*Geosciences and Environmental Change Science Center, U.S. Geological Survey, Denver, CO*

²*Mechanical Engineering and Materials Science, Yale University, New Haven, CT*

³*Department of Geosciences, The Pennsylvania State University, University Park, PA*

⁴*School of Earth and Sustainability, Northern Arizona University, Flagstaff, AZ*

Corresponding Author's Email: jfitz@usgs.gov

CONTENTS OF THIS FILE

Figure S-1 Examples of chessboard subgrains in the SDM-A, GISP2-D, and SPICE cores

S-1 Data re-sampling and potential error sources

S-2 Characterization of uncertainties

Figure S-2 Determination of the dispersion value for low strain grains in the sample 805 VTS

Figure S-3 Determination of the dispersion value for the low strain grain in the sample 1325 VTS

Figure S-4 Characterization of SGBs in sample 1325 VTS

S-3 Characterization of additional chSGBs in all samples

Figure S-5 Characterization of chSGBs in sample 805 VTS; Grain CH-1

Figure S-6 Characterization of chSGBs in sample 805 VTS; Grain CH-2

Figure S-7 Characterization of chSGBs in sample 805 VTS; Grain CH-3

Figure S-8 Characterization of chSGBs in sample 1125 VTS; Grain CH-2

Figure S-9 Characterization of chSGBs in sample 1325 VTS; Grain CH-1

INTRODUCTION

This Supplemental Information file contains additional text, RGB imagery, and analyses related to the characterization of SGBs and chSGBs observed in the WAIS Divide ice core.

DATA POLICY

The complete set of data used in this manuscript is available via download at Fitzpatrick, Joan J., Wilen, Larry, Voigt, Donald, Alley, Richard, and Fegyveresi, John, 2024, Data release for Characteristics, origin, and significance of chessboard subgrain boundaries in the WAIS Divide Ice Core: U.S. Geological Survey data release, <https://doi.org/10.5066/P1CPP6YN>

Fig. S-1 Examples of chSGBs in SDM-A, GISP2-D, and SPICE cores.

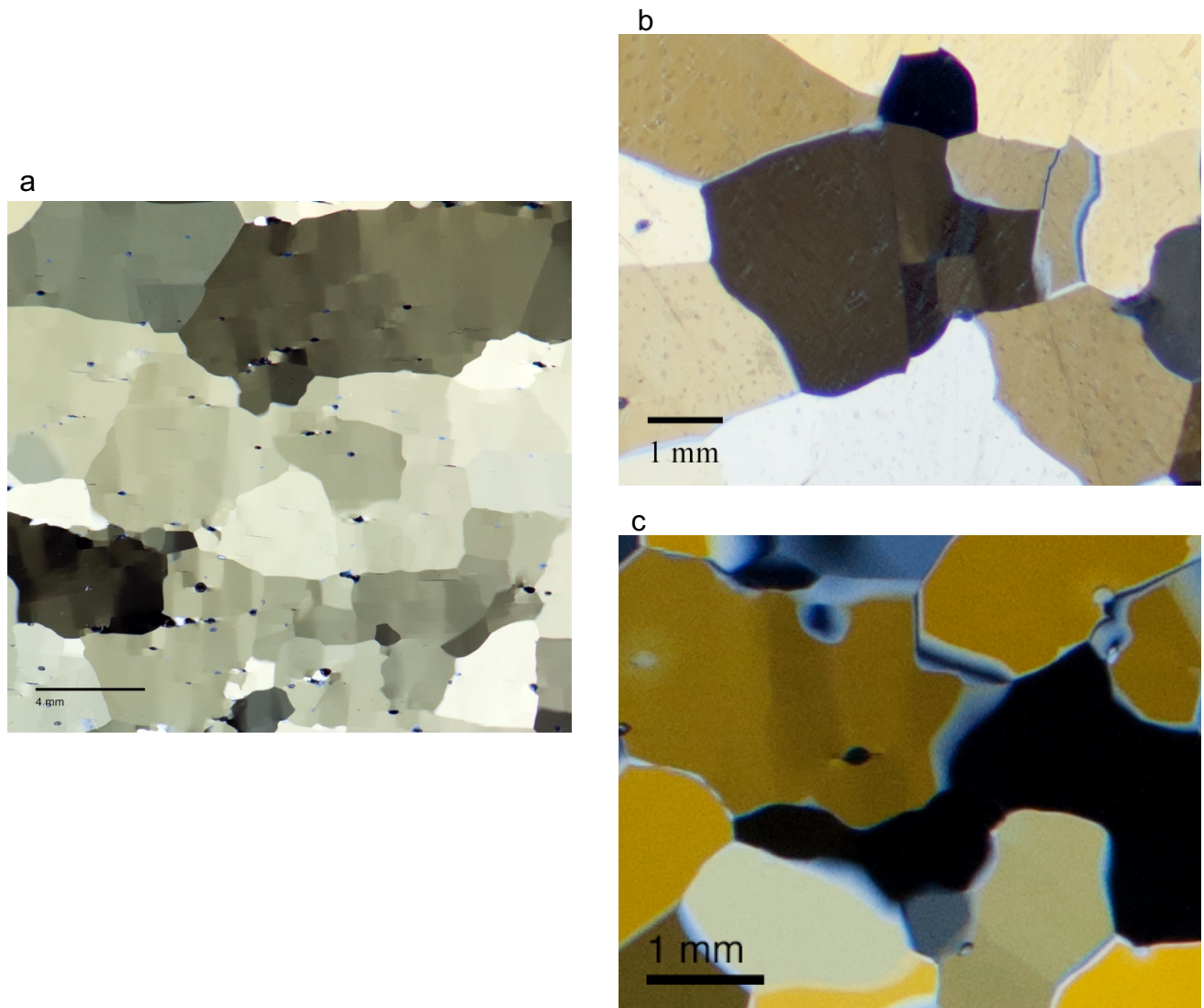


Fig. S-1 Chessboard subgrains in the (a) Siple Dome A core (SDM-A, 759 m), (b) GISP 2D core (953 m), and (c) the South Pole ice core (SPICEcore, 500m) (Photo credit for SDM-A Samantha Barnett, Northern Arizona University)

S-1 Data re-sampling and potential error sources

The automated technique used for determining c-axis orientations is as described in Hansen and Wilen (2002), but with some small modifications. For analyzing grains in a thin section, the original method was to find the 2-dimensional center of mass of a grain (or in the case of an oddly shaped grain, some other point well in the grain interior) and use a 3x3 pixel region centered on that point to generate extinction curves from images of the section as crossed polarizers were rotated. The extinction angles found from

these curves with the thin section positioned in 9 different orientations (one reference image with the section perpendicular to the optic axis determined by the 2 polarizers, and 8 images with the section at 45 degrees to this axis) allowed the determination of the *c*-axis orientation for each grain. A mapping function allowed the same spatial region to be used to generate the extinction curve for each orientation of the thin section. In this study, we reduced the size of the region used to generate the extinction curve to a single pixel in the reference image. This single pixel was then mapped (with the same mapping function) to corresponding single pixels in all the thin section orientations. There are several consequences of this modification. First, the extinction curves could be noisier since the light level is determined from a single pixel in contrast to an average of 9 pixels. Second, the spatial resolution of the *c*-axis location was higher but was not increased by a factor of 3 for the following reasons: a typical grain boundary that is roughly perpendicular to the thin section plane will have a spatial extent of up to $\sqrt{2}/2$ times the ice thickness when the thin section is oriented by 45 degrees, which is the angle used for 8 of the 9 extinction curves. Hence, the abruptness in the change of *c*-axis orientation with position cannot be measured to a resolution higher than the spatial extent of this angled grain boundary. In fact, the consequences may be more subtle because an extinction curve generated from light passing through more than one grain, which is the case for a pixel sitting over an angled boundary, can yield an ambiguous extinction angle or a very low contrast extinction curve. The analysis will usually throw away such curves, and in most cases that grain (i.e. pixel) will not yield a result. On the other hand, if the two grains have very similar orientations, the analysis will often yield a result, but it is likely to be somewhere between the two *c*-axes; again, the spatial resolution would be reduced.

Another possible source of error in the spatial resolution is due to small errors in the mapping from one section orientation to another. This error is typically of order 1-2 pixels as measured in the reference image. Due to the above effects, the error in *c*-axis direction, and the spatial resolution were checked carefully as discussed in the main body text. These checks determined the ultimate spatial resolution in practice.

S-2 Characterization of uncertainties

To characterize the orientation uncertainty, resampled datasets were generated on three sets of low-strain grains. These grains were assumed to lack high concentrations of dislocations causing misorientation and therefore should exhibit a low average point-to-point misorientation (Lu and others, 2003). Size and orientation information for these grains is given in **Table 1**.

Analyses of low strain grains are shown in **Figs. 4, S-2 and S-3**. The observed dispersions are close to the uncertainty of the original orientation measurements for the fabric analysis system as described in Hansen and Wilen, 2002 ($\pm 0.25^\circ$). Single-pixel traverses were also constructed for the low-strain grains in each sample to set appropriate significance levels for single-pixel traverses run on grains in the same thin section with conventional and chessboard SGBs. Dispersion values were calculated on the basis of the first pixel in the row/column of analysis.

For consistency, we report both spatial and angular values at the highest level of precision, which is that of the high-resolution RGB imagery. We interpret orientation changes as being significant only when they are larger than the dispersion values of the low-strain grains in the same sample as the chSGBs being measured.

Fig. S-2 Determination of the dispersion value for low strain grains in 805 VTS

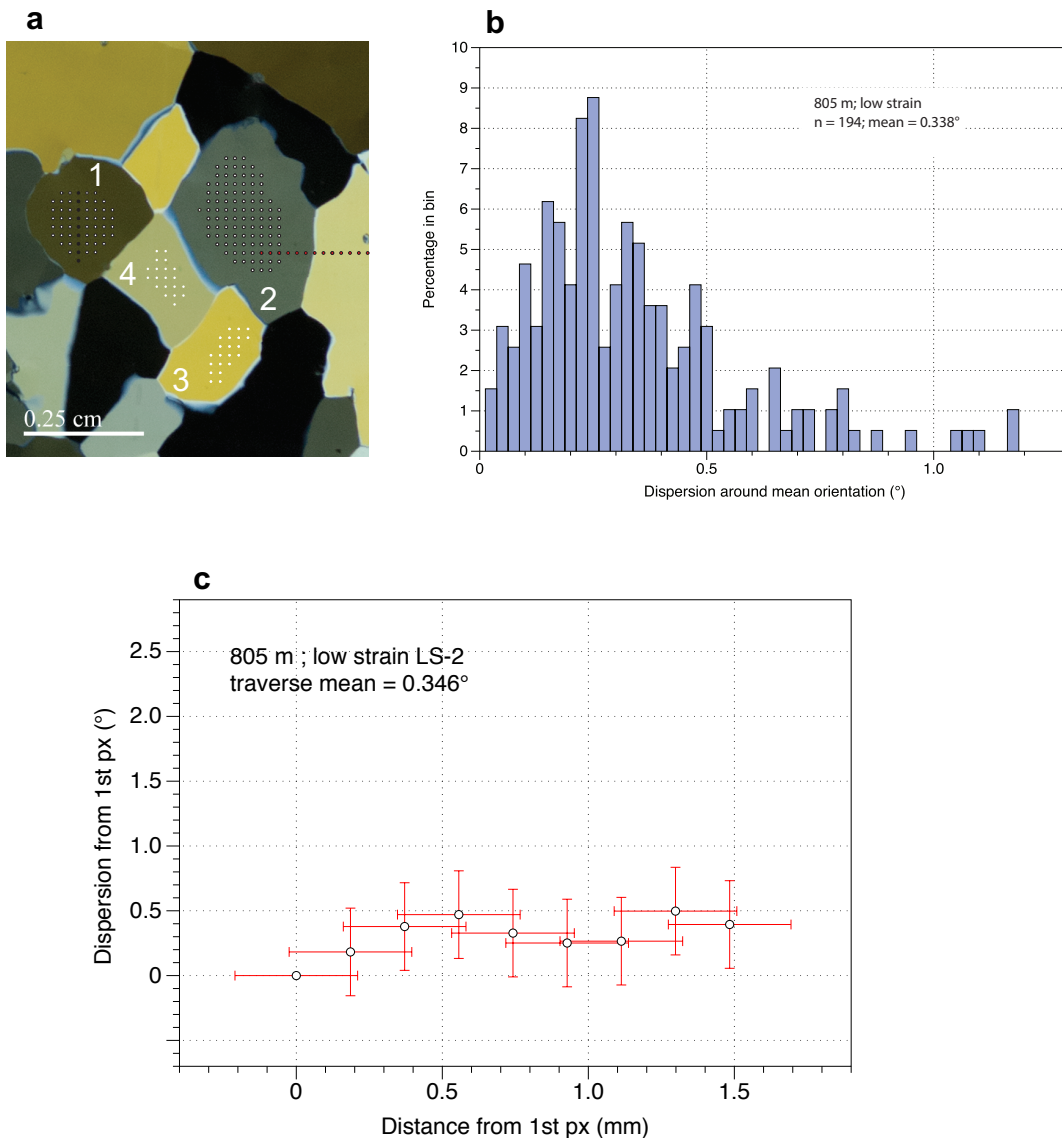


Fig. S-2 A set of low-strain grains identified in sample 805 VTS used for characterizing angular uncertainty in c -axis measurements. (a) RGB image of grains in thin section with pixel center locations for orientation analyses overlaid (white dots). Red dots identify the location of pixels used for the high-angle grain boundary traverse shown in **Fig. 5** in the main body text. (b) The distribution of the dispersions of c -axis orientations around the vector mean for each grain. (c) Single-pixel traverse across leftmost low-strain grain (LS-1).

Fig. S-3 Determination of the dispersion value for low strain grains in sample 1325 VTS.

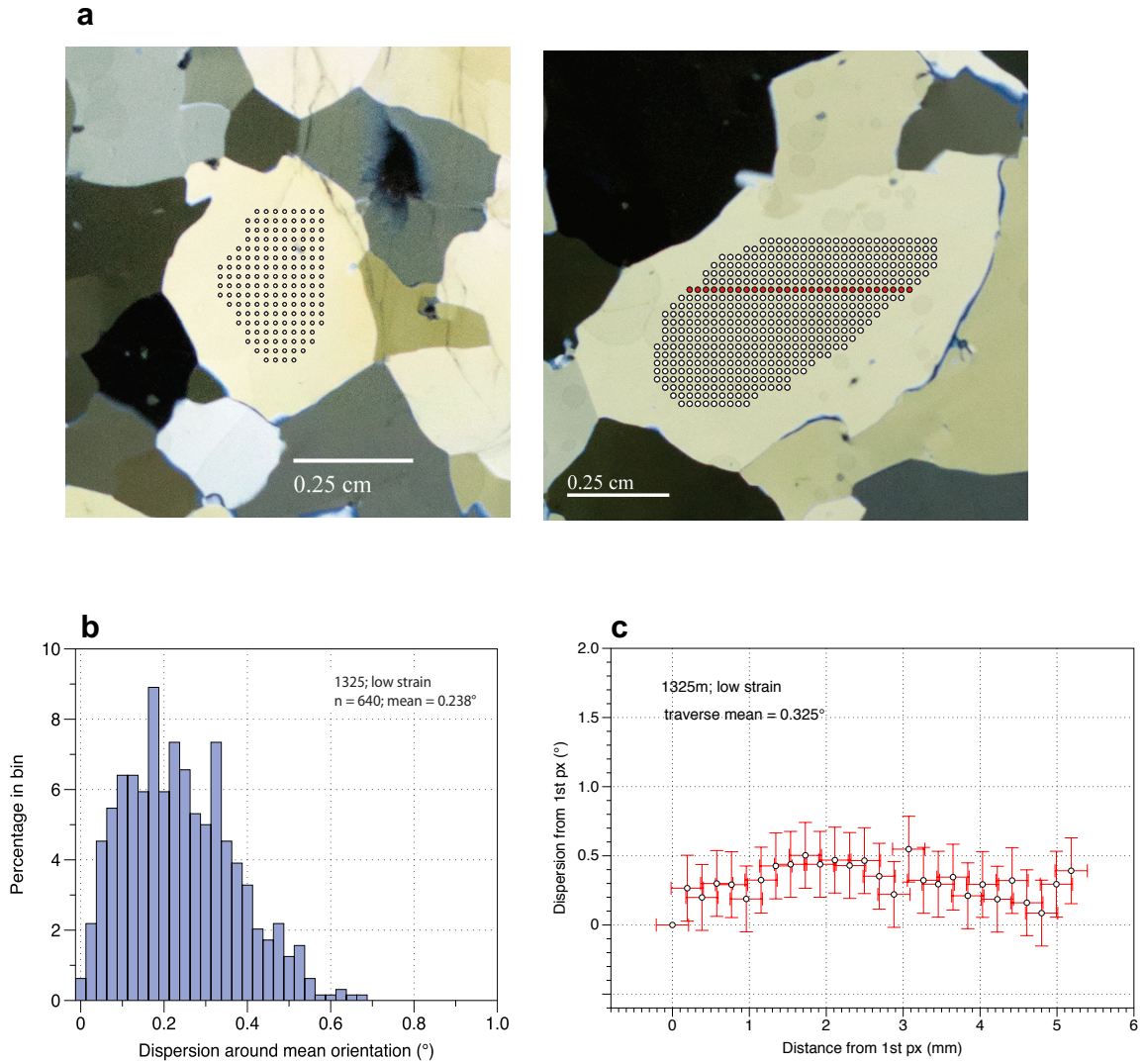


Fig. S-3 Low strain grains identified in sample 1325 VTS. (a) White dots are pixel-center locations for single-pixel orientation analyses. *c*-axis orientations were determined at a total of 640 points over two grains. (b) The distribution of the dispersions of *c*-axis orientations around the mean for each grain. (c) Dispersion traverse across right grain (red dots).

Fig. S-4 Characterization of SGBs in sample 1325 VTS.

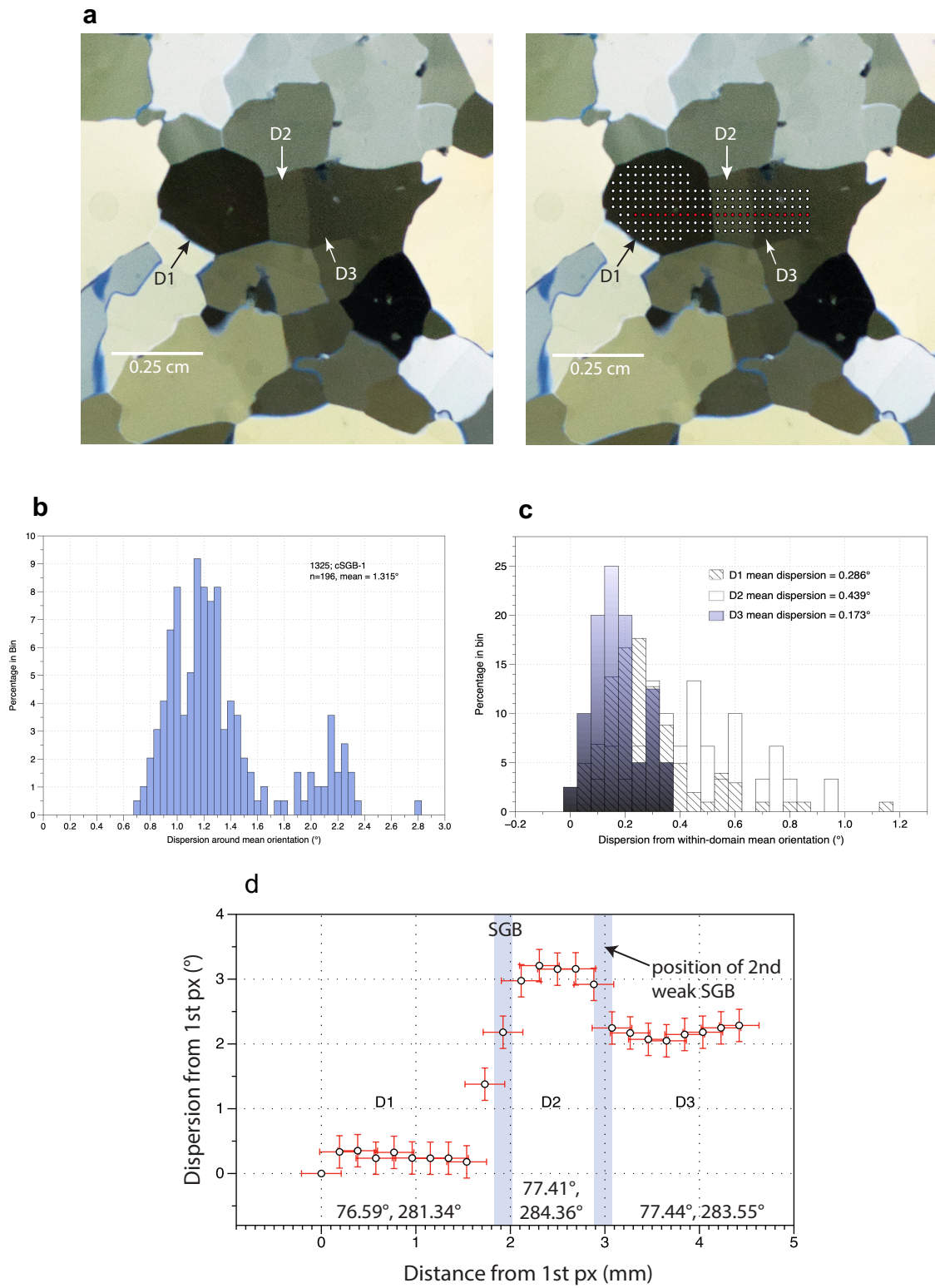


Fig. S-4 Sample 1325 VTS, grain SGB-3, conventional subgrain domain boundaries. (a) RGB thin section image and overlay of 196 pixel-center locations used for orientation analyses (white dots) and the position of a horizontal traverse line across subgrain boundaries (red dots). Subgrain boundary traces are perpendicular to the trace of (0001). (b) Dispersions around the mean of all observations. (c) Within-domain dispersions (d) Single-pixel traverse dispersions across the subgrain boundaries (red dots). Dispersion values are calculated from the orientation of the leftmost pixel. The means for the segregated domains are shown at the bottom of the plot. The orientation change across the D1-D2 subgrain boundary calculated from the mean orientations on either side of it is 3.06° ; across the weak D2-D3 subgrain boundary it is 0.79° . The D1-D2 subgrain boundary shows 2-px wide ramp as the boundary is approached from the left side and a slight deflection within the uncertainty approaching from the right. The D2-D3 boundary shows slight deflections from both sides, but they are within the uncertainty of the measurements.

S-3. Characterization of additional chSGBs in all samples

Sample 805 VTS

Single-pixel *c*-axis orientation data are provided on three grains in this sample, CH-1, CH-2, and CH-3, each of which contain bubbles and chessboard domains. Pertinent information on grain size and mean orientation are given in **Table 2**.

Chessboard grain 805 CH-1

A 101-pixel region around two bubbles on the left side of grain 805 CH-1 (**Fig. S-5a**) was examined in detail. Bubbles at this depth are slightly flattened in the (0001) plane (Fitzpatrick and others, 2014; Fegyveresi and others, 2016). Both the apparent direction of bubble flattening in the image and the mean grain *c*-axis orientation (75.19° , 255.21°) are consistent with the trace of domain walls of the chessboard patterns lying approximately parallel and perpendicular to the trace of the basal (0001) crystallographic plane in the vicinity of the bubble. The trace (0001)-normal chSGB extending between the two bubbles appears to deflect toward the trace (0001) chSGB associated with the lower of the two bubbles.

The *c* axis is inclined at about 15° to the plane of the sample, which is a less-favorable geometry than other grains examined in this study. The distribution of the orientation dispersions calculated on the mean of all 101 points is shown in **Fig. S-5b**. The mean orientation dispersion is 1.042° , which is approximately 3 times larger than the orientation dispersion mean for the low-strain grains in the same sample (0.338°).

A single-pixel traverse across the (0001)-normal chSGB trace separating the left and right subgrain domains D1 and D2 (**Fig. S-5c**) indicates an asymmetric ramp in the orientation change as the subgrain boundary is approached. D1 orientation approaching the subgrain boundary from the left is not stable within the uncertainty of the measurement and changes continuously up to the boundary. D2 orientation between the bubbles is stable and displays no ramp into the subgrain boundary within the uncertainty of the measurement. Because the mean *c*-axis orientation of this grain is significantly inclined to the plane of the thin section, interpretation of the behavior of the θ (polar) and φ (azimuthal) angles as the subgrain boundary is crossed is

problematic; however, a mean orientation change of 1.32° across the subgrain boundary can be calculated based on orientation values for pixels residing within each of the subgrain domains delineated by the chSGBs. This orientation change lies within the range of misorientations observed across conventional SGBs and is larger than the mean misorientation observed in the low-strain traverse in the same sample.

Fig. S-5 Characterization of chSGBs in sample 805 VTS; Grain CH-1

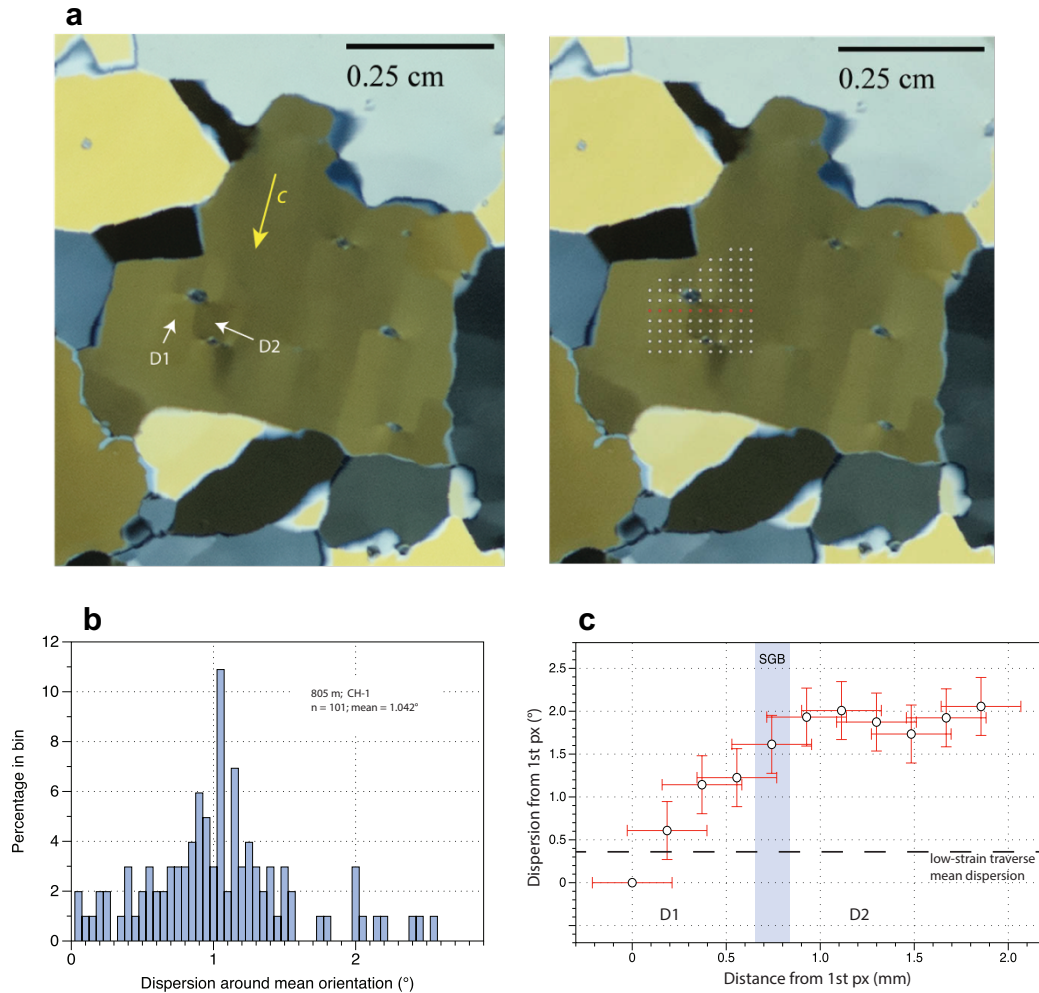


Fig. S-5 Single-pixel orientation analysis for chessboard grain 1 (CH-1) in sample 805 VTS. (a) (left) RGB thin section image and (right) overlay of pixel-center locations for 101 orientation analyses. (b) Distribution of orientation dispersions around the mean orientation for the entire dataset. (c) c -axis orientation change as the trace (0001)-normal chessboard subgrain boundary trace separating D1 and D2 is crossed. Traverse location is row of red dots in (a), right. Dispersion values are calculated as the deviation from the leftmost pixel.

Chessboard grain 805 CH-2

An 99-pixel region around the only bubble in this grain was examined in detail (**Fig. S-6a**). As with grain CH-1, the subgrain boundary traces in this grain also appear to lie along (0001) and the perpendicular to (0001). Because the *c*-axis of this grain lies much closer to the plane of the thin section than that of grain CH-1, the subgrain boundaries are considerably clearer in this image. This grain has a complex subgrain domain structure and at least 7 subgrain domains separated by both chSBs and conventional SGBs can be distinguished by inspection of the grain image.

The distribution of the orientation dispersions calculated on the mean of all 99 orientation values is shown in **Fig. S-6b**. The mean dispersion (0.601°) is approximately 1.8 times larger than the orientation dispersion mean for the low-strain grains in the same sample (0.338°) and slightly smaller than the smallest dispersion value observed for conventional SGBs. The combination of small grain size, low resolution, and complex microstructure precludes having a sufficient number of pixels within single domains to produce a meaningful characterization of each SGB for this grain; however, a traverse across the long dimension of the grain can provide some insight into the trends in orientation change behavior as three trace (0001)-normal chSGBs and two possible conventional (no bubble association) (0001)-normal SGBs are crossed (**Fig. S-6c**). Small but systematic changes in *c*-axis orientation can be detected at each SGB crossing after averaging the within-domain dispersions (dark bars in **Fig. S-6c**), but only the orientation changes for domains D2, D4, and D6 lie outside the uncertainties from the mean dispersion measured on the low-strain traverse in the same sample.

Fig. S-6 Characterization of chSGBs in sample 805 VTS; Grain CH-2

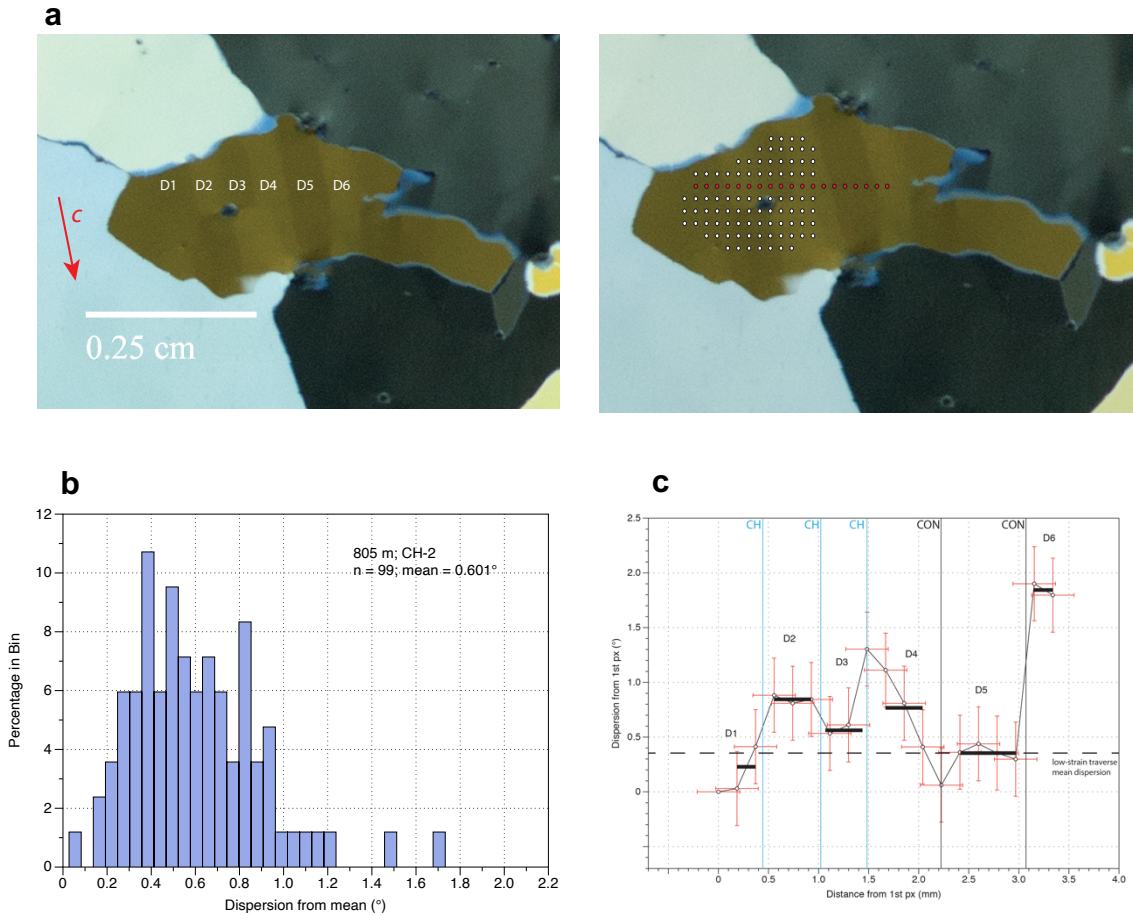


Fig. S-6 Chessboard grain CH-2 in sample 805 VTS. (a) RGB thin section image (left) and overlay of 99 single-pixel orientation analysis locations (right). (b) Distribution of orientation dispersions around the mean orientation for the entire dataset. (c) Left-to-right traverse across the long dimension of this grain (red pixel centers) crosses a complex of three chessboard (0001)-normal trace boundaries associated with the single bubble in the grain and two possible conventional subgrain boundaries. Orientation changes are averaged within domains (heavy lines) and locations where subgrain boundaries cross the traverse line are indicated as thin lines for clarity and are actually 1-px wide. Dispersion values are calculated as the deviation from the leftmost pixel.

Chessboard grain 805 CH-3

A 103-pixel region around the large bubble close to the center of this grain was examined in detail (**Fig. S-7a**). Chessboard-style subgrain domain walls sub-parallel and perpendicular to the trace of the (0001) plane can be seen around the bubble and, as observed in chessboard grains CH-1 and CH-2, the subgrain domain boundaries that are perpendicular to the trace of (0001) are consistently longer than the domain boundaries that lie parallel to the trace of (0001).

The mean of all 103 single-pixel dispersions (**S-7b**) is 1.089° . This is 3.2 times larger than the mean dispersion for low-strain grains in the same sample.

Single-pixel traverses crossing both the (0001) and (0001)-normal type chSGB traces in this grain show orientation changes of 2.60° and 2.83° , respectively (**Fig. S-7c-d**). These values lie within the range of misorientations observed across conventional SGBs in the same sample. A 1-px wide ramp can be seen crossing the (0001) chSGB from D1 into D2 in **Fig. S-7c**. No ramp is detected approaching the boundary from the D2 side. A 1-px-wide ramp is observed when approaching the (0001)-normal chSGB from both D2 and D3 in **Fig. S-7d**. In both cases, subgrain domain orientations appear to be stable within the uncertainty of the measurement on either side of the chSGBs.

Fig. S-7 Characterization of chSGBs in sample 805 VTS; Grain CH-3

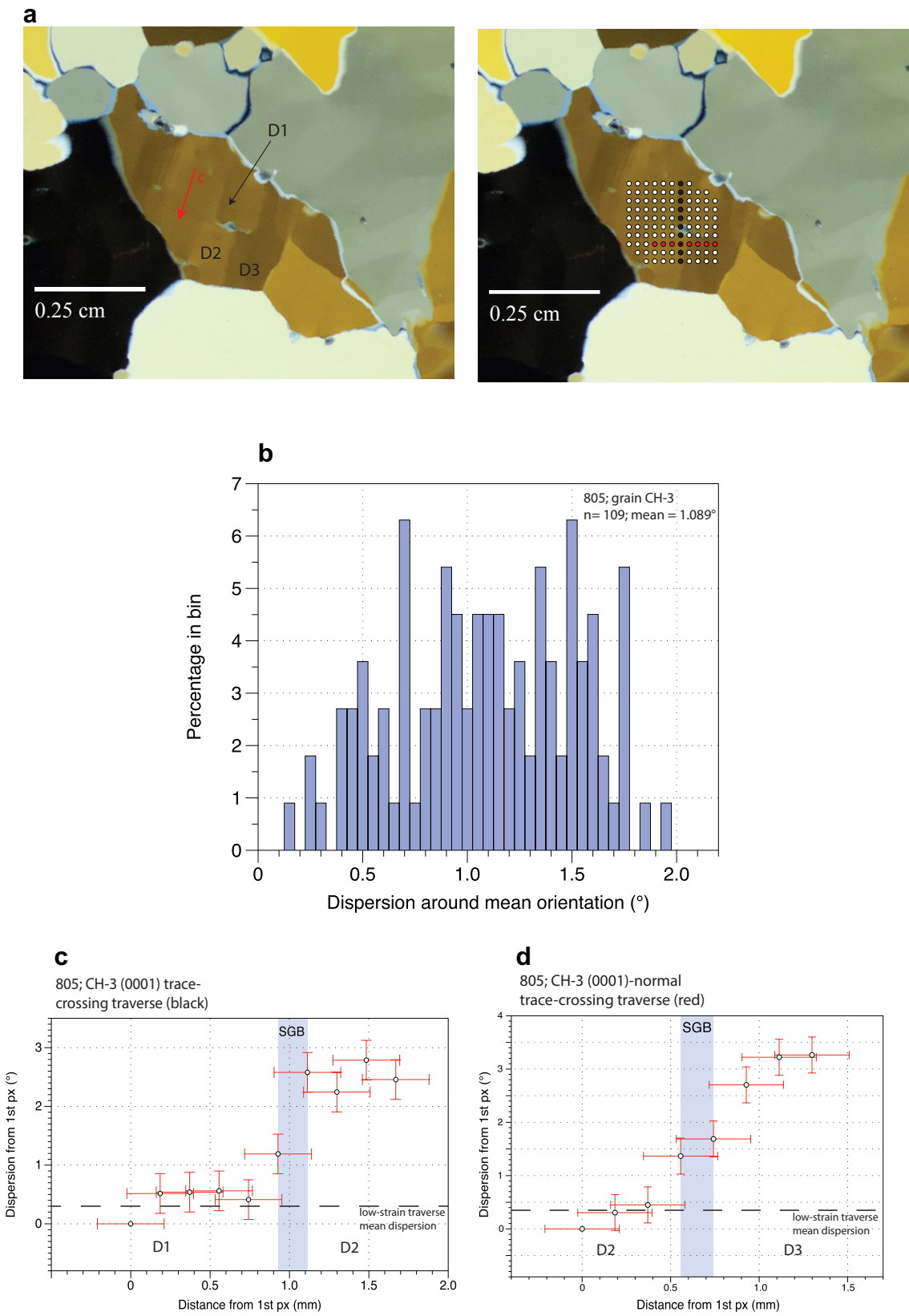


Fig. S-7 Chessboard grain CH-3 in sample 805 VTS. (a) RGB thin section image (left) and overlay of 109 single-pixel orientation analysis locations (right). Red and black pixels indicate the position of single-pixel traverses in (c) and (d). Zero values for these traverses are the uppermost and leftmost pixels (b) Distribution of orientation dispersions around the mean orientation for the entire dataset. (c) Single-pixel traverse across chSGB parallel to the trace of the (0001) , (d) Single pixel traverse across chSGB perpendicular to the trace of the (0001) crystallographic plane.

Chessboard grain 1125 CH-2

This large grain is segmented into two large subgrain domains that are heavily chessboarded (**Fig. S-8a**). The large SGB that divides the grain is subparallel to the trace of the (0001)-normal chSGBs. The mean orientation change across the large SGB, based on two sets of single-pixel arrays situated inside the subgrains (**Fig. S-8b**), is 2.2° , a value which, when combined with the configuration of the SGB extending from one HAGB to another, argues for it being a conventional SGB rather than a chSGB.

The mean of the distribution of all single-pixel orientation dispersions from the overall mean grain orientation is 1.45° (**Fig. S-8b**), approximately four times larger than that of the low-strain grains in this sample. As with grain CH-1 in this sample, the population distribution is clearly bimodal across the conventional SGB. Mean dispersion value for the D1 domain alone (**Fig. S-8c**) is comparable to the mean dispersion value of the low-strain grain in the same sample. Mean dispersion for the D2 domain is approximately 1.5 times higher.

Fig. S-8 Characterization of chSGBs in sample 1125 VTS; Grain CH-2

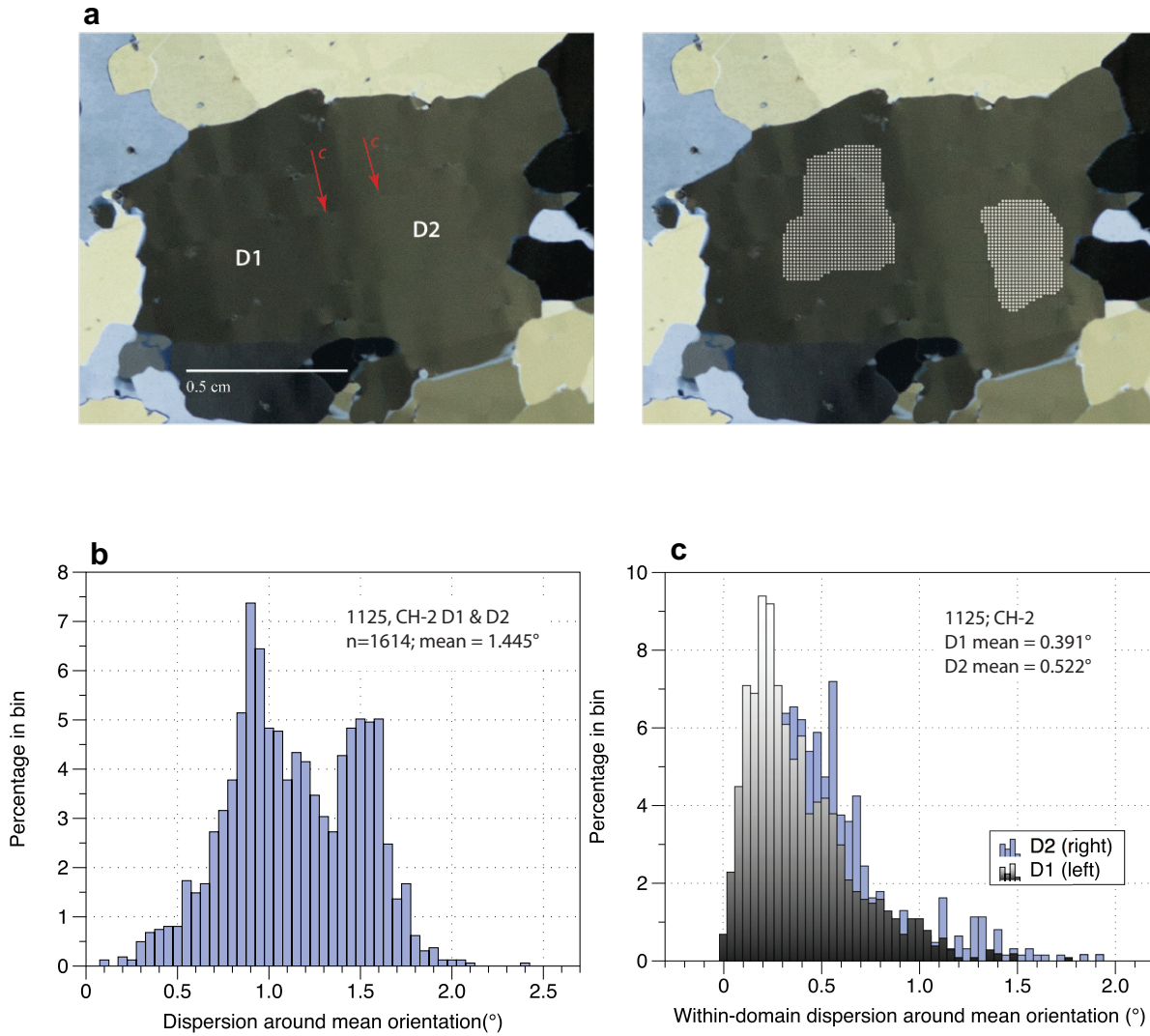


Fig. S-8 Chessboard grain CH-2 in sample 1125 VTS. (a) RGB thin section image (left) and overlay (right) of 1002 (D1) and 612 (D2) pixel-center locations used for orientation analyses. (b) Histogram of the distribution of orientation dispersions around the mean orientation for the entire dataset. (c) Distributions of orientation dispersions within each of the chessboarded domains.

Sample 1325 VTS

Chessboard grain 1325 CH-1

This grain is somewhat unfavorably oriented for chSGB characterization as the *c*-axis is inclined at about 16° to the plane of the sample resulting in a distortion of the appearance of the subgrain domains. Multiple domains are visible in the RGB image, and a 316 single-pixel array was constructed to investigate the orientation distributions and transitions across the chSGBs (**Fig. S-9a**).

The mean of the single-pixel orientation dispersions is 0.92°, 3.8 times larger than that of low strain grains in the same sample (**Fig. S-9b**). The orientation changes observed crossing a (0001) chSGB trace and a (0001)-normal chSGB trace have somewhat different characteristics. As observed in most other instances, chSGBs occurring in the (0001)-normal configuration are generally longer than those occurring in the trace (0001) configuration. The orientation change along a single-pixel column traverse crossing a trace (0001) subgrain boundary (black pixel-column in **Fig. S-9a**) is 0.79° (**Figure S-9c**). Although a 1-px deflection is observed approaching the boundary from either direction, it is within the uncertainty of the measurement. The domain orientations are stable on either side of the boundary.

The orientation change along a single-pixel row traverse crossing a trace (0001)-normal chSGB (red pixel row in **Fig. S-9a**) shows an orientation change of 2.23°, nearly 3 times the orientation change observed crossing the basal chSGB. Although the orientation is stable on either side of this boundary (**Fig. S-9d**), a longer ramp exists (~5 px) than is typically observed in shallower samples. This is possibly due to a combination of the shallow inclination of the boundary to the plane of the sample that is suggested by its diffuse appearance in the RGB image and the unfavorable inclination of the *c*-axis to the plane of the sample.

Fig. S-9 Characterization of chSGBs in sample 1325 VTS; Grain CH-1

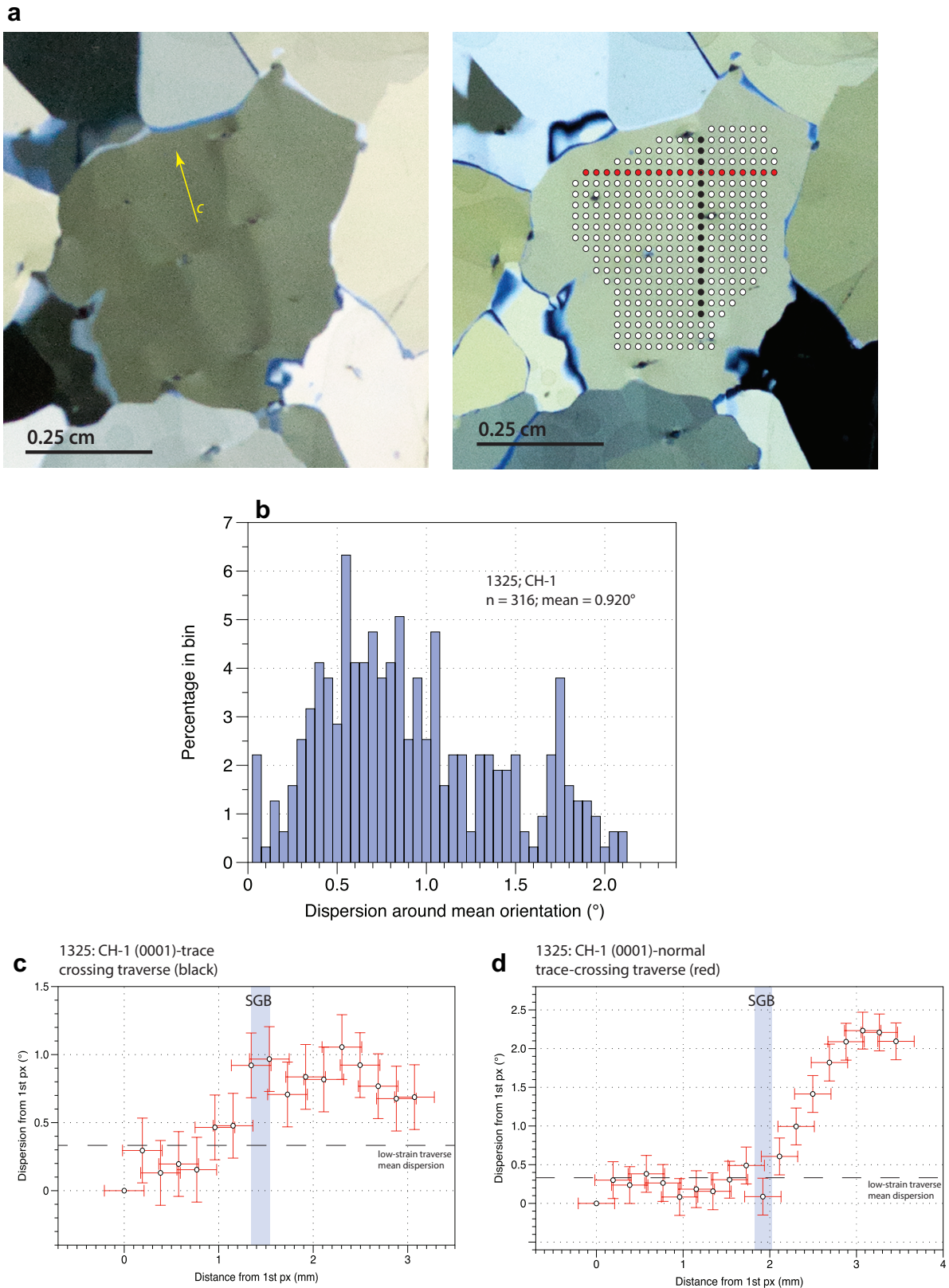


Fig. S-9 Chessboard grain CH-1 in sample 1325 VTS. (a) RGB thin section image (left) with 316 pixel-center locations (right) used for orientation analyses superimposed. (b) Histogram of the distribution of orientation dispersions around the mean orientation for the entire dataset. (c) Single-pixel traverse across a (0001) chSGB trace in the center part of the grain (black dots). (d) Single-pixel traverse across a (0001)-normal chSGB trace at the top of the grain (red dots).